Electrochimica Acta 259 (2018) 841–849

Contents lists available at ScienceDirect

Electrochimica Acta

journal homepage: www.elsevier.com/locate/electacta

Sandwich-like $Cu_{2-x}Se@C@MoSe_2$ nanosheets as an improved-performance anode for lithium-ion battery

Rencheng Jin*, Xiguang Liu, Lixia Yang, Guihua Li, Shanmin Gao**

School of Chemistry & Materials Science, Ludong University, Yantai, 264025, PR China

ARTICLE INFO

Article history:
Received 26 September 2017
Received in revised form
7 November 2017
Accepted 7 November 2017
Available online 8 November 2017

Keywords:
Transition metal selenides
Nanosheets
Sandwich-like structure
Anodes
Lithium-ion battery

ABSTRACT

Transition metal chalcogenides are considered as promising materials for lithium-ion battery, however, the application in practical devices is still hampered by their poor cycling performance and rate capability. In this work, we design and construct sandwich-like $Cu_{2-x}Se@C@MoSe_2$ nanosheets to enhance the cycling and rate performances of $Cu_{2-x}Se$. The reversible capacity could be retained at 432 mAh g^{-1} after 100 cycles at the current density of 100 mA g^{-1}. At 2000 mA g^{-1}, the specific capacity still retains at 163 mAh g^{-1}. The improved lithium storage performance can be attributed to its structural features, which enhance the electrical conductivity, buffer the volume change as well as increase their structural stability during cycling.

1. Introduction

Rechargeable lithium-ion batteries (LIBs) have been considered as the dominant power source due to its potential application in various electric vehicles [1–4]. With the increasing requirement for safer power and higher capacity, the commercial graphite anode has been extremely prohibited for its low theoretical capacity (372 mAh g^{-1}) [5,6]. Therefore, searching new anode materials to replace the graphite becomes urgent. In this aspect, copper chalcogenides are considered as the promising candidates due to their low cost, good electrical conductivity and high capacity [7–9]. Unfortunately, rapid capacity fading originated from drastic volume expansion/contraction still hampers its application in practical Li-ion devices. Although some strategies such as doping foreign atom [10] and constructing nanostructured electrodes [11,12] are adopted to improve the electrochemical performance, the considerable capacity fading still can be observed.

Recently, two-dimensional (2D) nanostructures have been attractive extensive attention because of their unique structural properties and surface characteristics [13]. However, the facet of the 2D nanostructures is smooth and the aggregation and stacking easily generate during the Li^+ intercalation and deintercalation process [14]. The tight aggregated nanoplates or nanosheets can not only reduce the contact area between the electrode and the electrolyte, but also elongates ion diffusion paths, which inhibit their practical application potential in energy storage. To solve this issue, constructing loosely stacked sandwich like architectures by employing additional additives is an effective route. Stimulated by this concept, numerous sandwich like 2D architectures are synthesized and evaluated as anode for LIBs [15–20]. Unfortunately, most of these 2D frameworks are mainly limited to graphene nanosheet and the synthetic processes are complex. Therefore, exploring a facile and reliable synthetic procedure to fabricate sandwich-like 2D nanostructures without graphene is extremely crucial.

Molybdenum diselenide with lamellar crystal structure is of great interest in Li^+ storage because its crystal structure favors the intercalation/extraction of Li ions [19,21–24]. Like transition metal oxides hybrids electrodes, the synergistic effect between copper selenides and molybdenum diselenide is expected to enhance the electrochemical performance for LIBs. Herein, $Cu_{2-x}Se@C@MoSe_2$ nanosheets were synthesized by a facile glucose-assisted solvothermal method via $Cu_{2-x}Se@C$ as template. Due to the unique sandwich-like structure and the composition, the as-prepared $Cu_{2-x}Se@C@MoSe_2$ hybrids exhibit excellent cycling performance (436 mAh g^{-1} after 100 cycles at 100 mA g^{-1}) and high rate capacity (163 mAh g^{-1} after 50 cycles at 2000 mA g^{-1}).

* Corresponding author.
** Corresponding author.
E-mail addresses: jinrc427@126.com (R. Jin), gaosm@ustc.edu (S. Gao).

https://doi.org/10.1016/j.electacta.2017.11.044
0013-4686/

2. Experimental section

2.1. Synthesis of $Cu_{2-x}Se$@C nanosheets

All the reagents were analytical grade and used without further purification. In the typical process, 0.2 g of copper acetate monohydrate, 0.1 g sodium selenite and 0.9 g of glucose were dispersed into the 18 mL of mixed solution (the volume ratio of water to isopropanol is equal to 3:15). After being stirred for 10 min, 0.3 g of sodium hydroxide and 2 mL of hydrazine hydrate (80%) were added into the above solution in turn. The mixture was transferred into 25 mL of Teflon-lined stainless steel autoclave and kept at 180 °C for 12 h. The sample was collected, washed with distilled water and dried at 80 °C for 8 h. For the preparation of the $Cu_{2-x}Se$@C nanosheets, a facile hydrothermal process was carried out. 0.1 g of $Cu_{2-x}Se$ nanosheets and 0.15 g glucose were dispersed into 15 mL of distilled water and ultrasonically treated for 10 min. Then the solution was sealed and held at oven at 180 °C for 6 h. After the autoclave was cooled naturally to room temperature, the sample was collected and labeled as $Cu_{2-x}Se$@C.

2.2. Synthesis of $Cu_{2-x}Se$@C@$MoSe_2$ nanosheets

0.15 g of the as-prepared $Cu_{2-x}Se$@C nanosheets was firstly immersed into 10 mL of distilled water and constantly stirred for 10 min. Then 0.087 g ammonium molybdat, 0.06 g of sodium selenite, 0.3 g of glucose, and 10 mL of ethylene glycol were introduced into above solution. After being ultrasonically treated for 30 min, 1 mL of hydrazine hydrate was added into the mixture. After solvothermal treatment at 180 °C for 12 h, the black precipitate was fabricated. Finally, the black products were washed with distilled water and dried at vacuum at 100 °C overnight for further characterization.

2.3. Materials characterization

XRD patterns were collected on Rigaku D/Max-2550pc X-ray diffractometer with Cu Kα radiation in the 2θ range of 10°–80°. The morphology of the obtained samples was detected on field-emission scanning electron microscope (SEM, FEI Quanta 200F). Transmission electron microscopy (TEM) and the high-resolution TEM (HRTEM) were detected on a Tecnai G2 S-Twin microscope with an energy-dispersive X-ray spectrometer operating at 20 KV. X-ray photoelectron spectroscopy (XPS) was performed on a PHI-5702 multifunctional X-ray photoelectron spectrometer. The composition of the obtained product was determined on inductively coupled plasma (ICP, NexION 300). The nitrogen gas adsorption/desorption isotherms were measured on Micromeritics ASAP 2460 instrument.

2.4. Electrochemical measurements

To prepare the working electrodes, the obtained active materials, carbon black (conductive agent), and polyvinylidene fluoride (PVDF, polymer binder) were firstly dispersed in N-methyl pyrrolidinone (NMP) with a weight ratio of 70:15:15. The homogeneous slurry was spread on the clean copper foil and dried in the vacuum at 100 °C for 12 h. The mass loading of active material on the current collector was approximately 2 mg cm^{-2}. The electrochemical performance was measured by using CR2025 coin type cells, which were assembled in an argon-filled glovebox. The electrolyte was composed of 1 mol L^{-1} $LiPF_6$ in a mixture of ethylene carbonate and diethyl carbonate (V_{EC}:V_{DEC} = 1:1), Celgard 2400 was used as the separator, and the Li-metal foil acted as the counter and reference electrode. All discharge and charge measurements were characterize on NEWARE CT3008 battery test system at different current densities in the potential range of 0.01–3.0 V. Cyclic voltammetry tests were carried out by a CHI660E electrochemical workstation at a scan rate of 0.2 mV s^{-1}. Electrochemical impedance spectroscopy (EIS) was detected on the same electrochemical workstation at frequencies ranging from 100 kHz to 0.01 Hz.

3. Results and discussion

The $Cu_{2-x}Se$@C@$MoSe_2$ is synthesized through three steps. In the first step, the $Cu_{2-x}Se$ is prepared by a simple solvothermal process. The $Cu_{2-x}Se$@C is subsequently fabricated through hydrothermal method using glucose as carbon source (step II). The crystallographic structure and phase purity of the $Cu_{2-x}Se$@C are characterized by XRD. As presented in Fig. 1, all the diffraction peaks can be indexed to the cubic $Cu_{2-x}Se$ (JCPDS card no. 06–0680). After solvothermal treatment in the presence of ammonium molybdat and sodium selenite (step III), the strong peaks assigned to $Cu_{2-x}Se$ can also be apparently observed. Meanwhile, some tiny peaks can also be found, which are attributed to $MoSe_2$ (JCPDS card no. 29–0914).

The morphology and structure of the $Cu_{2-x}Se$@C are characterized by SEM, TEM and HRTEM. As can be seen in Fig. 2a, the obtained samples are composed of numerous nanosheets. The thickness of the $Cu_{2-x}Se$@C is approximately 20–50 nm (Fig. 2b). Fig. 2c presents the low magnification TEM image of the $Cu_{2-x}Se$@C, uniform nanosheets can be clearly observed, which is in accordance with the SEM image (Fig. 2a). The HRTEM image clearly displays the crystalline nature of these $Cu_{2-x}Se$@C nanosheets (Fig. 2d), and the observed lattice fringe of 0.335 nm corresponds to the (111) plane of cubic $Cu_{2-x}Se$. In addition, the $Cu_{2-x}Se$ nanosheets are tightly wrapped by a thin layer of amorphous carbon.

Fig. 3a depicts the SEM image of the $Cu_{2-x}Se$@C@$MoSe_2$. Compared with $Cu_{2-x}Se$@C, the surface of the nanosheets becomes coarse and numerous nanoparticles are uniformly distributed on the $Cu_{2-x}Se$@C nanosheets. The high magnification SEM image further confirms that $MoSe_2$ and Se nanoparticles with the average diameter of 13 nm are homogeneously dispersed on $Cu_{2-x}Se$@C nanosheets to form a three dimensional sandwich structure (Fig. 3b). The corresponding TEM image reveals the successful formation of $MoSe_2$ and Se nanoparticles on the surface of $Cu_{2-x}Se$@C nanosheets (Fig. 3c). Interestingly, the surface of the $Cu_{2-x}Se$@C@$MoSe_2$ possesses a two dimensional porous architecture (Fig. 3d). More features of the crystallographic structures of the Cu_{2-}

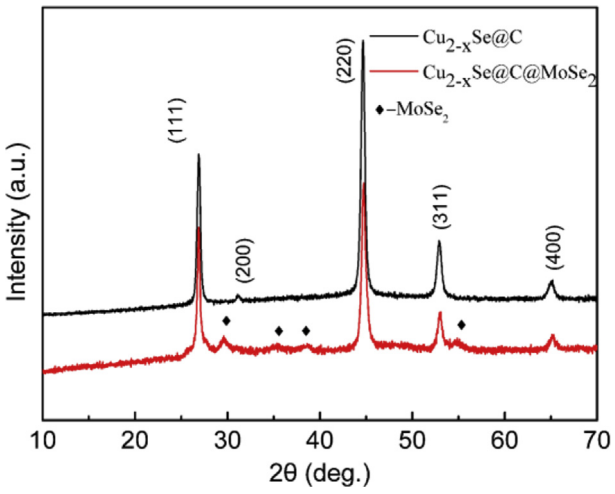

Fig. 1. XRD pattern of $Cu_{2-x}Se$@C and $Cu_{2-x}Se$@C@$MoSe_2$ nanocomposites.